AAPS PharmSciTech (2019) 20: 274
DOI: 10.1208/s12249-019-1486-9

Research Article

Insight into the Dissolution Molecular Mechanism of Ternary Solid Dispersions by Combined Experiments and Molecular Simulations

Run Han,[1] Tianhe Huang,[1] Xinyang Liu,[1] Xunqing Yin,[2] Haifeng Li,[2] Jiahong Lu,[1] Yuanhui Ji,[3] Huimin Sun,[4] and Defang Ouyang[1,5]

Received 25 February 2019; accepted 18 July 2019; published online 5 August 2019

Abstract. With the increase concern of solubilization for insoluble drug, ternary solid dispersion (SD) formulations developed more rapidly than binary systems. However, rational formulation design of ternary systems and their dissolution molecular mechanism were still under development. Current research aimed to develop the effective ternary formulations and investigate their molecular mechanism by integrated experimental and modeling techniques. Glipizide (GLI) was selected as the model drug and PEG was used as the solubilizing polymer, while surfactants (*e.g.*, SDS or Tween80) were the third components. SD samples were prepared at different weight ratio by melting method. In the dissolution tests, the solubilization effect of ternary system with very small amount of surfactant (drug/PEG/surfactant 1/1/0.02) was similar with that of binary systems with high polymer ratios (drug/PEG 1/3 and 1/9). The molecular structure of ternary systems was characterized by differential scanning calorimetry (DSC), infrared absorption spectroscopy (IR), X-ray diffraction (XRD), and scanning electron microscope (SEM). Moreover, molecular dynamic (MD) simulations mimicked the preparation process of SDs, and molecular motion in solvent revealed the dissolution mechanism of SD. As the Gordon–Taylor equation described, the experimental and calculated values of Tg were compared for ternary and binary systems, which confirmed good miscibility of GLI with other components. In summary, ternary SD systems could significantly decrease the usage of polymers than binary system. Molecular mechanism of dissolution for both binary and ternary solid dispersions was revealed by combined experiments and molecular modeling techniques. Our research provides a novel pathway for the further research of ternary solid dispersion formulations.

KEY WORDS: solid dispersion; dissolution effect; molecular modeling; ternary system.

INTRODUCTION

It is reported that most of new active pharmaceutical ingredients (APIs) found and synthesized in recent years exist poor aqueous solubility (1,2). Approximately 40% percent active compounds belonged to the Biopharmaceutics Classification System (BCS) class II (3,4). To solve this problem, many techniques are applied to increase solubility, and one of the most popular formulations is amorphous solid dispersion (SD) (5,6). In recent years, more and more studies investigate molecular mechanism of SDs, and more medicinal products with SD technique were approved by FDA (7). APIs interact with one or more excipients to form amorphous form by the solubilization effect of polymer (8). Compared with traditional binary SD systems with single polymer, ternary systems with the addition of third component exhibit more significant solubilization effect. In general, ternary system contains drug molecules with two different polymers, or with one polymer and one surfactant. Table I summarizes the components of ternary systems with surfactants. Usually, the weight ratio of surfactants has accounted to 10–20% in majority of ternary formulations. However, 10–20% surfactant in the formulation may be too much as the toxicity of surfactants. On the other hand, the molecular mechanism of SDs is also unclear although SD technique has been developed for five decades. The interaction between drug and polymer could change physical chemical properties and even influence *in vivo*

[1] State Key Laboratory of Quality Research in Chinese Medicine, Institute of Chinese, Medical Sciences (ICMS), University of Macau, Macau, China.
[2] Institute of Applied Physics and Materials Engineering, University of Macau, Macau, China.
[3] Jiangsu Province Hi-Tech Key Laboratory for Bio-medical Research, School of Chemistry and Chemical Engineering, Southeast University, Nanjing, 211189, China.
[4] National Institute for Food and Drug Control, No. 2, Tiantan Xili Road, Beijing, 100050, China.
[5] To whom correspondence should be addressed. (e–mail: defangouyang@umac.mo)

Table I. The compositions of ternary solid dispersion in published papers

Drug	Polymer	Surfactant	Reference
Dipyridamole (DPM)	Polyvinyl pyrrolidone (PVP)	Sodium dodecyl sulfate (SDS) poloxamer 188	(9)
	Hydroxy propyl methyl cellulose (HPMC)	Sodium dodecyl sulfate (SDS) poloxamer 188	
Cinnarizine (CNZ)	Polyvinyl pyrrolidone (PVP)	Sodium dodecyl sulfate (SDS) poloxamer 188	
	Hydroxy propyl methyl cellulose (HPMC)	Sodium dodecyl sulfate (SDS) poloxamer 188	
Valsartan (VAL)	Polyethylene glycol 6000 (PEG 6000)	Poloxamer 407 (PLX 407) Stearoyl macrogol-32 glycerides (Gelucire 50/13)	(10)
Praziquantel (PZQ)	Polyvinyl pyrrolidone (PVP)	Poloxamer	(11)
Naproxen (NAP)	Polyvinyl pyrrolidone co-vinyl acetate 64 (PVP VA 64)	D-α-tocopheryl polyethylene glycol 1000 succinate (TPGS) Capryol 90 Lauroglycol FCC	(12)
Acetaminophen (APAP)	Polyvinyl pyrrolidone co-vinyl acetate 64 (PVP VA 64)	D-α-tocopheryl polyethylene glycol 1000 succinate (TPGS) Capryol 90 Lauroglycol FCC	
Ezetimibe (EZ)	Polyvinyl pyrrolidone K30 (PVP K30)	poloxamer 188	(13)
Itraconazole	PVPVA HPMCAS	Sodium lauryl sulfate (SLS) D-α-tocopheryl polyethylene glycol 1000 succinate (TPGS)	(14)
	Eudragit	D-α-tocopheryl polyethylene glycol 1000 succinate (TPGS)	
	Soluplus	Sodium lauryl sulfate (SLS)	
Griseofulvin (GF)	Hydroxypropyl cellulose (HPC)	SDS	(15)
Itraconazole (ITZ)	Polyethylene glycol (PEG)	Glyceryl dibehenate Stearoyl macrogol-32 glycerides (Gelucire 50/13)	(16)
Phenytoin Griseofulvin Probucol	Polyvinyl pyrrolidone (PVP)	SDS	(17)
Olmesartan medoxomil (OLM)	Polyvinyl pyrrolidone K30 (PVP K30)	Poloxamer 407 (PLX 407)	(18)
Gliclazide (GLIC)	Polyethylene glycol 6000 (PEG 6000)	Pluronic F-68 (PL F-68)	(19)
Diacerein (DIA)	Polyethylene glycol 4000 (PEG 4000) Polyethylene glycol 6000 (PEG 6000)	Pluronic F-68 (PL F-68)	(20)
Daidzein (DZ)	Polyvinyl pyrrolidone K30 (PVP K30)	Poloxamer (PLX)	(21)
Ibuprofen (IBU)	Hydroxy propyl methyl cellulose (HPMC) Hydroxy propyl cellulose (HPC) Kollicoat IR Kollidon VA 64	Poloxamer 407 (PLX 407)	(22)
Spironolactone (SPIR)	Hydroxy propyl methyl cellulose (HPMC) Hydroxy propyl cellulose (HPC) Kollicoat IR Kollidon VA 64	Poloxamer 407 (PLX 407)	(23)
Novel Tanshinone II A (TA)	Polyvinyl pyrrolidone	Ploxamer 188	(24)
Tacrolimus (FK 506)	Hydroxy propyl methyl cellulose (HPMC)	Sodium lauryl sulfate (SLS) Gelucire 50/13 Vit E TPGS	(25)
Ketoprofen (KETO)	Polyethylene glycol 15000 (PEG 15000)	Sodium dodecyl sulfate (SDS) Dioctylsulfosuccinate (DSS) Tween 60	(26)
Anti-HIV drug UC 781	Eudragit E100	D-tocopheryl polyethylene glycol succinate 100 (TPGS 100)	(27)
Glyburide (GLY)	Polyethylene glycol 6000 (PEG 6000)	Sodium lauryl sulfate (SLS) Tween 80 Cremophor RH40	(28)
Itraconazole (ITRA)	Polyvinyl pyrrolidone co-vinyl acetate 64 (PVP VA 64)	D-tocopheryl polyethylene glycol succinate 1000 (TPGS 1000)	(29)

Table I. (continued)

Drug	Polymer	Surfactant	Reference
Anti-HIV drug UC 781	Polyvinyl pyrrolidone co-vinyl acetate 64 (PVP VA 64) Hydroxy propyl methyl cellulose 2910 (HPMC 2910)	D-tocopheryl polyethylene glycol succinate 1000 (TPGS 1000)	(30)
Itraconazole (ITRA)	Polyvinyl pyrrolidone co-vinyl acetate 64 (PVP VA 64)	Myrj 52	(31)
Naproxen (NAP)	Polyethylene glycol 4000 (PEG 4000)	Sodium dodecyl sulfate (SDS) Tween 80	(32)
	Polyethylene glycol 6000 (PEG 6000)	Sodium dodecyl sulfate (SDS) Tween 80	
	Polyethylene glycol 20,000 (PEG 20,000)	Sodium dodecyl sulfate (SDS) Tween 80	
Ezetimibe (EZE) and lovastatin (LOV) in a fixed dose combination (FDC), co-amorphous systems	Soluplus®	Tween 20 Tween 80 Gelucire 44/14 Cremophor RH40 TPGS	(33)
Fenofibrate	Poloxamer 188	TPGS	(34)
Sulfathiazole	PVP K29/32	Sodium lauryl sulfate (SLS)	(35)
Ketoprofen	PVP K30	Tween 80	(36)

performance of drugs, which still need to be further elucidated. With the development of computer science, the novel computational technique could be applied in pharmaceutical research to assist and reveal dissolution molecular mechanism of SD.

Molecular modeling is a powerful technique to integrate quantum mechanics theory and computational methods to investigate molecular structure (37). It could mimic the behavior of molecules at atomic level based on the molecular mechanics and quantum chemistry theory. The potential functions and force parameters are described as force fields to calculate the force between interacted molecules and overall energy of whole system (37,38). Molecular modeling could provide visible three-dimensional structure and the trajectories profile. The parameters (*e.g.*, free energy and dynamic parameters) could be calculated from trajectories to reveal molecular structure (38). Because of unique advantages of molecular modeling, there are more and more application examples in pharmaceutical research (39). In the previous works of our group, the molecular structures of a serious of ibuprofen solid dispersions that interacted with PEG, poloxamer, PVP, lactose, and mannitol were exhibited by simulated annealing method (40), and the dissolution process of ibuprofen SDs with PEG, PVP, and poloxamer were also conducted by molecular dynamic simulation (41). For the ketoprofen-PEG system and its ternary system with surfactants, molecular modeling simulated their structures and dissolution process to investigate dissolution mechanism (42). Therefore, molecular modeling is an important tool that assists to explain experimental phenomenon at molecular level.

This study aims to develop the effective ternary SD system and investigate the dissolution mechanism at molecular level. Glipizide (GLI) was selected as the model drug (43). Amorphous SDs were prepared with hydrophilic polymer and very small amount of surfactant to improve the dissolution of GLI. Differential scanning calorimetry (DSC), infrared spectroscopy (IR), X-ray diffraction (XRD), scanning electron microscope (SEM), dissolution test, and molecular modeling were applied to characterize SDs and mimic the molecular structure and reveal dissolution molecular mechanism at atomic level.

MATERIALS AND METHODS

Materials

GLI was purchased from Wuhan Dongkang Technology Company Limited, China. Polyethylene glycol (PEG), sodium dodecyl sulfate (SDS), and tween 80 (TWE) were purchased from Beijing J&K Scientific Company Limited, China. All other chemicals used in the study were of analytical grade.

Experimental Part

Preparation of Amorphous Solid Dispersion

The ternary SD systems of GLI consist of GLI, PEG6000, and surfactants (*e.g.*, SDS and TWE) at the weight ratio of 1:1:0.02 (that means only 1% surfactants were added). In addition, three binary systems were also prepared at the ratio of 1:1, 1:3, and 1:9 as comparison group. Each component was accurately weighted as Table II list. After completely mixed, the SD samples were prepared by hot melting method. In the process of SD preparation, PEG need to be heated and maintained at 70–75°C to reach molten state. GLI was added into molten polymer with continuous stirring and mixed at least 5 min until a homogeneous system formed. For the ternary system, GLI and surfactant were firstly mixed completely and added into molten polymer. After that, the mixtures were instantly cooled down in the ice bath. The solid powder was pulverized and sieved to obtain glipizide solid dispersion samples (GLI-SD), then stored in sealed glass bottle for the following analysis.

Table II. The components of GLI-PEG SD

	The ratio of API (*w*/*w*)	GLI (mg)	PEG (mg)	SDS (mg)	TWE (mg)
GLI-PEG (1:1)	0.5	500	500	0	0
GLI-PEG (1:3)	0.25	500	1500	0	0
GLI-PEG (1:9)	0.1	500	4500	0	0
GLI-PEG-SDS	0.495	500	500	10	0
GLI-PEG-TWE	0.495	500	500	0	10

Physical mixtures (PMs) were obtained from homogeneous blending with GLI, PEG, and SDS or TWE. The weighted components were mixed and stored at anhydrous conditions as physical mixture.

Solubility Study

Firstly, the solubility of GLI need to be tested in five mediums with different pH value. Then, water and pH 7.4 phosphate buffer were selected as the solvents to compare solubility of drug and SDs. Solubility test for PM and GLI-SD samples were conducted by adding excess amount of GLI and GLI-SDs into 10 mL solvent to evaluate solubilizing ability of polymer. The sealed glass bottles with samples and solvent were sonicated for 10 min and shaken at 37°C for 72 h until the equilibrium. Solution samples were filtered through 0.45 μm syringe filter and determined by UV spectrophotometer at 276 nm.

Dissolution Study

Dissolution studies of GLI, PM, and GLI-SDs were performed at 37°C with a fully automated USP paddle Apparatus (Erweka DT700), and pH 7.4 phosphate buffer was used as dissolution medium. All samples with 10 mg of GLI were added into 900 mL pH 7.4 phosphate buffer with the stirring rate of 100 rpm. The 5-mL solution samples were collected through a 0.45-μm syringe filter for UV analysis at different time sets: 5, 10, 15, 20, 30, 45, and 60 min. An equal volume of pH 7.4 phosphate buffer was added into solution to maintain a constant volume of dissolution medium.

Differential Scanning Calorimetry (DSC)

DSC analysis was performed with DSC-60A to investigate thermodynamics behavior of GLI, polymer, PMs, and GLI-SD systems. The DSC cell was calibrated with indium under 50 mL/min of nitrogen flow. Approximately 5-mg samples were weighted into the aluminum pan sealed with aluminum lid. The thermal analysis was conducted at the heating rate of 10°C/min over the temperature range of 30–300°C in nitrogen atmosphere. Meanwhile, the blank aluminum pan was used as the control group. From the resulting thermal map, the melting temperature (T_m) of GLI and thermodynamic peaks of amorphous SD systems were reported.

To investigate the effect of Tg, the thermal behavior of all SDs was examined by DSC using a series of heating-cooling-heating cycles. Samples were heated at 10°C/min from 30 to 300°C (cycle 1), then cooled at a rate of 10°C/min to 30°C (cycle 2), and then reheated at 10°C/min from 30 to 300°C (cycle 3). In addition, a heating rate of 2°C/min was used to ensure that a single Tg occurred regardless of the constant heating rate.

Fourier Transform Infrared Spectroscopy (FT-IR)

FT-IR spectrum of GLI, PEG, surfactants, PMs, and GLI-SD systems were recorded by PerkinElmer Frontier. All samples were grinded with KBr to get the fine powder and compressed as a thin tablet individually. The process undergone with the wavelength scan range of 40–4000 nm at the resolution of 2 cm^{-1}. Meanwhile, the pure KBr thin tablet is treated as the blank reference.

Powder X-ray Diffraction (XRD)

XRD study of GLI, PEG, surfactants, PMs, and GLI-SD samples was performed on an in-house diffractometer (SmartLab 9KW). It employed the copper $K\alpha_1$ (λ = 1.54056 Å) and $K\alpha_2$ (λ = 1.54439 Å) with $I\alpha_1/I\alpha_2 = 0.5$ as the radiation and a 2θ step size of 0.004° s^{-1} at a voltage of 45 kV. The current of 200 mA and ambient conditions to explore the structural crystal property.

Scanning Electron Microscope (SEM)

SEM images of GLI, PEG, surfactants, PM, and GLI-SD systems were obtained by the ZEISS Sigma. All samples were gold sputter-coated to conduct them electrical. SEM investigation was performed under an accelerating voltage of 2.00 kV in vacuum and with 5.00KX magnification.

Molecular Modeling Technique

The binary system GLI-PEG (1:1) and ternary SD systems (GLI-PEG-surfactant, 1:1:0.2) were conducted by AMBER 14 and AMBERTOOL 14 software package. General Amber Forcefield (GAFF) was applied in molecular dynamic simulation.

Molecular Structure Building

The molecular structure of GLI, PEG, SDS, and TWE was built by Discovery Studio Visualizer 4.5 (DSV), as shown in Fig. 1. The molecular structure of PEG was composed of 20 repeat ethylene glycol monomers. As for SDS segment, the sodium ion was added in the LEAP module in AmberTools 14. TWE was a polymer of ethylene oxide with an average degree of substitution. The geometries of all structures were optimized using a fast, Dreiding-like force field to ensure the lowest energy.

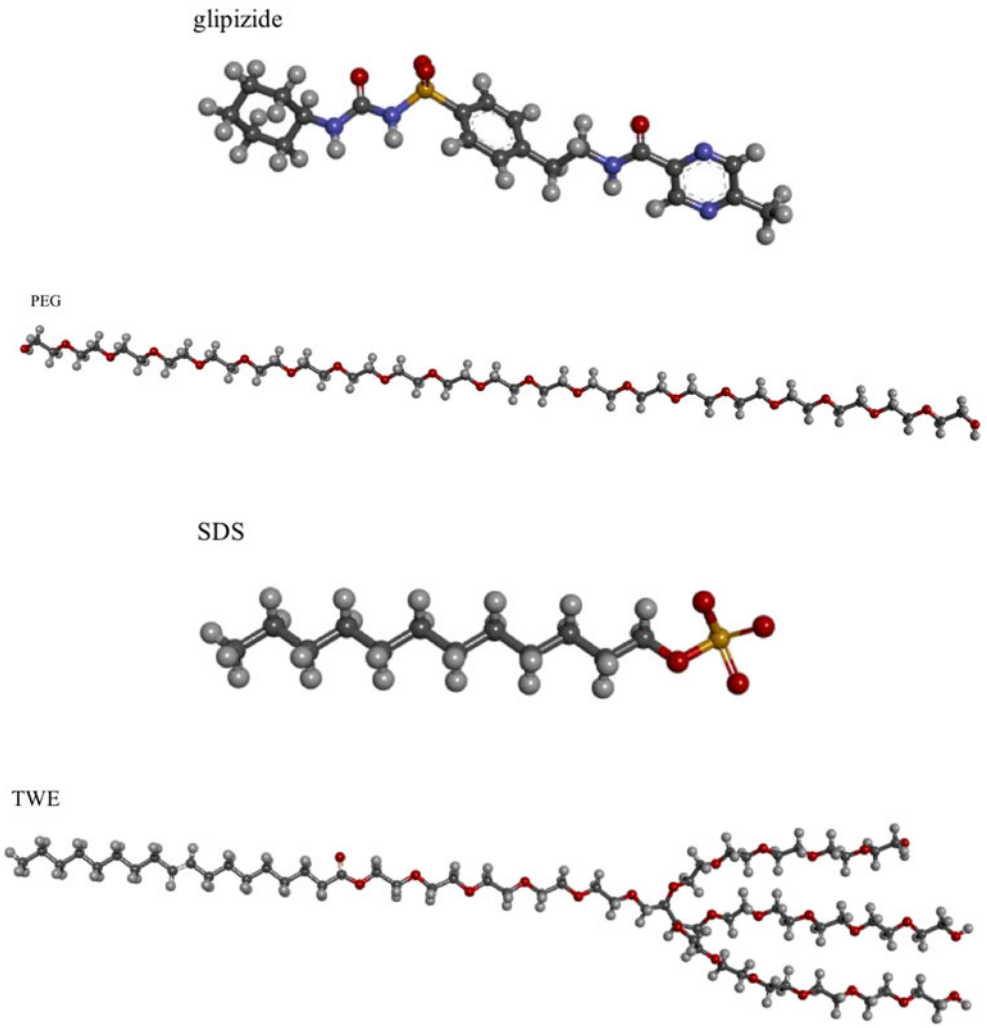

Fig. 1. The molecular structure of GLI, PEG, and surfactants

The molecular number of three SD systems were designed as Table III according to experimental formulations. All molecules of each SD system were loaded into Packmol program individually to build initial structure, and then transformed into LEAP module with GAFF in AmberTools 14 for further study.

Modeling for SD Preparation

Simulated annealing was an algorithm to find approximating optimal solution in a large search scale. The method simulated physical process of heating a material and then slowly lowering the temperature to minimize the system energy (44). In this study, the simulated annealing method was applied to mimic melting method in experimental part for the SD preparation. According to the previous research of our group (42), firstly, all the systems were conducted 1000 steps of the steepest descent minimization, and then got on 1000 steps of conjugate gradient minimization. After energy minimization, the whole system was gradually heated from 0 to 338 K during 200 ps and kept this temperature for 1800 ps to equilibrate the system. Then, all the systems were quickly cooled down from 338 to 273 K during 200 ps and kept 273 K for 1800 ps to reach equilibrium. In the simulation process, the Langevin dynamics was used to control the temperature with the collision frequency of 2 fs and the cut-off of 10 Å (40,42). Finally, the structures of SD systems were obtained.

Table III. The molecular number of SD systems in molecular modeling

SD system	GLI	PEG	SDS	TWE
GLI-PEG (1:1)	30	15	0	0
GLI-PEG-SDS (1:1:0.02)	30	15	1	0
GLI-PEG-TWE (1:1:0.02)	30	15	0	1

Molecular Dynamics Simulation for Dissolution Test

According to the dissolution experiments, the dissolution medium was pH 7.4 phosphate buffer solution. Solvated system was built by TIP3P model and the concentration of salt ion was set to 0.15 to ensure pH was 7.4. The structure of three systems was loaded into LEAP modules with GAFF, and each system was immersed in 30 Å solvation box individually for dissolution simulation. The solvent and ion

system were subjected 2000 steps of steepest descent minimization, followed by 2000 steps of conjugate gradient minimization under constant volume periodic boundaries to fix solute molecules in the system and minimize the positions of water and ions. Then, the minimization program was worked on the whole system for total 5000 steps. After two-stage minimizations, the whole system was heated from 0 to 300 K for total 10,000 steps with weak restraint. The control of temperature was realized by Langevin equilibration scheme. In the dissolution process, the simulation of three systems was performed for 300 ns with 2 fs per step and 10 Å cut-off.

RESULT AND DISCUSSION

Solubilization Effect of SDs

Solubility Study

As a weakly acidic drug, the solubility of GLI relates to the solvent pH values as shown in Table IV. It was worthy to note that the solubility of GLI in pH 7.4 phosphate buffer was about 40 times than that in pure water. Water as the most commonly used solvent and pH 7.4 phosphate buffer as the best solvent were used as medium to study the solubilization effect of SDs. SD samples showed better solubilization effect than PMs. The solubilization effect of PMs was caused by the hydrophilic properties of polymer, while that of SD contains not only the hydrophilic effect but also the interaction between drug and polymer or surfactants. In comparison with the binary system (SD 1:1), ternary systems with the addition of 1% surfactants showed the obvious increase of solubility in water. For ternary systems, SDS is an anionic surfactant, which is different from the nonionic surfactant Tween80. In the solution environment, both the ionization process and wetting effect could improve the dissolution ability of SD system, while the nonionic surfactant TWE has only wetting effect to increase the solubility of SD powder. Therefore, ternary systems with few surfactants could significantly improve the solubility of GLI as the binary system with high polymer ratio (SD 1:3 or 1:9). There was no significant difference between GLI, PMs, and GLI-SDs in pH 7.4 phosphate buffer.

Dissolution of GLI and GLI-SD

As the best solubility existed in pH 7.4 PBS, the dissolution rate of all samples was conducted in this medium as Fig. 3 shows. Although the solubility of pure GLI in pH 7.4 PBS could reach a high level (221 μg/mL, Fig. 2b), the cumulative release rate of GLI within 60 min was only 6.61%. For PM samples, with the polymer ratio increases, the dissolution rate of binary PMs increases, reaching the maximum 60%. Ternary PMs with surfactants could improve dissolution rate to over 90%. On the other hand, ternary SD systems with surfactants (GLI-PEG-surfactant 1:1:0.02) reached above 85% within 5 min and over 90% after 10 min, which has significant improvement than binary system (SD 1:1) and similar as high ratio systems (1:3 and 1:9).

To evaluate the dissolution ability between PM and SD samples, f2 factor was also calculated. The cumulative dissolution of PM samples was set as reference value; the f2 for SD (1:1), SD (1:3), SD (1:9), SD (1:1 + SDS), and SD (1:1 + TWE) were 17.32, 1.78, 3.69, 33.74, and 50.36, respectively. The dissolution behavior between PMs and SDs was quite different, which confirmed that SD was more effective than simple PM. The molecular motions and interactions of SDs in the dissolution process were investigated by molecular dynamic simulation in next section (Fig. 3).

Table IV. Solubility of GLI in different mediums

Medium	Solubility (μg/mL)
Water	5.19
0.1 M HCl	2.42
pH 6.8 Phosphate buffer	58.05
pH 7.4 Phosphate buffer	221.00
Sodium carbonate	155.71

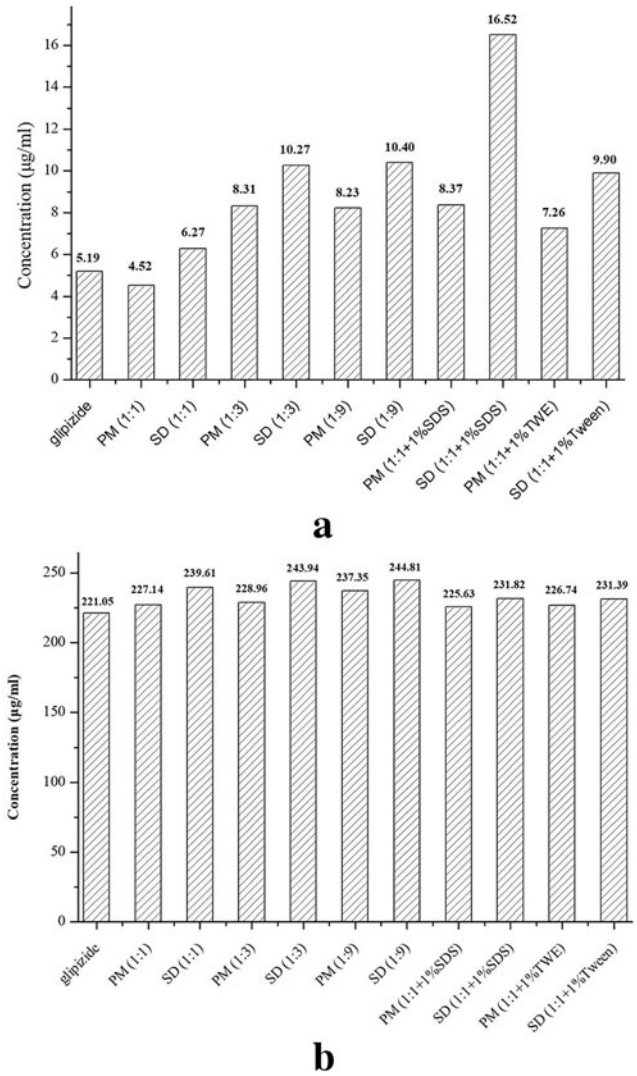

Fig. 2. Saturated solubility of GLI, PMs, and GLI-SDs in **a** H_2O and **b** PH7.4 phosphate buffer

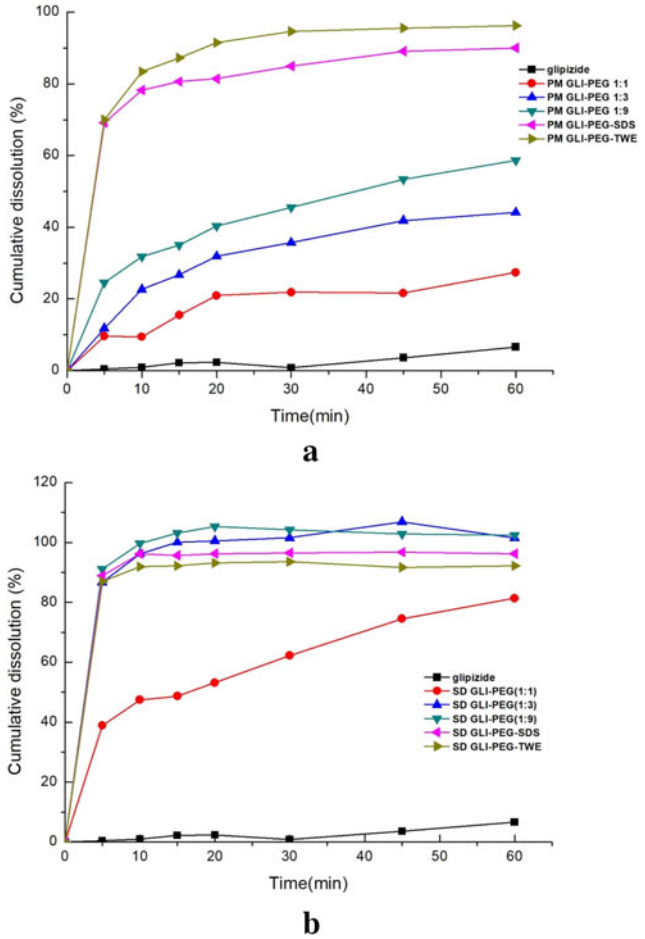

Fig. 3. Dissolution profile for **a** physical mixtures and **b** GLI solid dispersion in pH 7.4 phosphate buffer

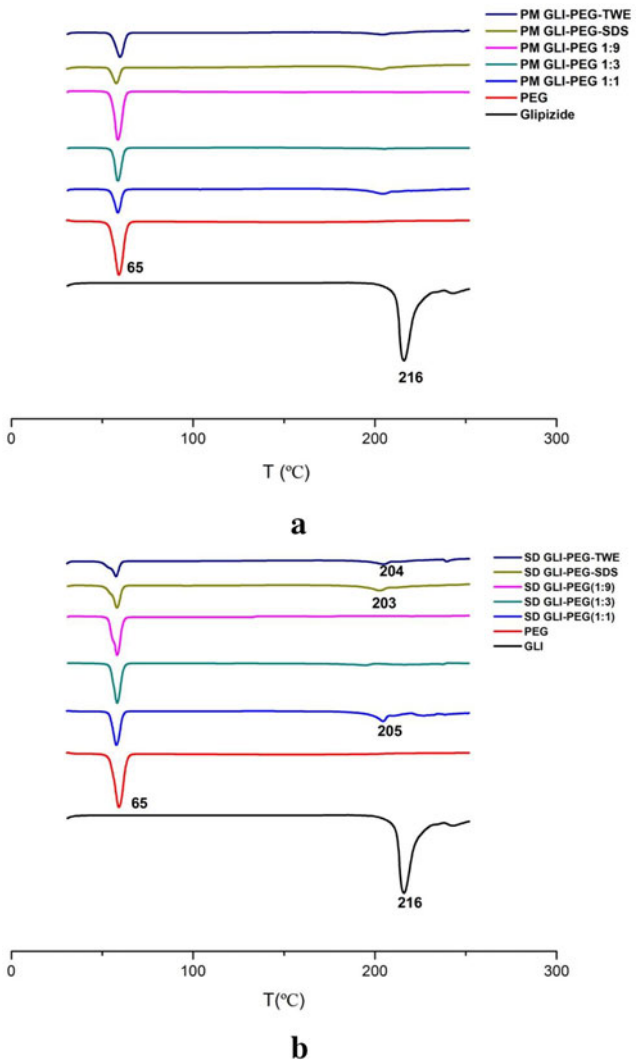

Fig. 4. DSC thermograms for **a** physical mixtures and **b** solid dispersions

The Structure Characterization Analysis for SDs

Differential Scanning Calorimetry for GLI and GLI-SD

DSC thermograms of five GLI solid dispersion systems are shown in Fig. 4. It was clear that a single sharp entomic peak was observed in GLI curve, which indicated the intrinsic melting point of GLI at 216°C. PEG also showed an endotherm at 65°C, respectively, with its melting properties. The sharp peak of GLI in all SD systems disappeared, instead of a small and broad peak. Glass transition temperature (Tg) existed in SD systems. In ternary systems, Tg was 129°C and 125°C for GLI-PEG-SDS and GLI-PEG-TWE SD individually, while that of binary systems was 145°C, 138°C, and 133°C for 1:1, 1:3, and 1:9 ratio, respectively. The Tg value showed the decreased tendency when the surfactants added, or the proportion of PEG increased. In addition, as Fig. 4 shows, a small broad endothermic peak existed in 178–233°C for GLI-PEG-SDS SD and 183–230°C for its PM sample, while it also viewed in 184–221°C for GLI-PEG-TWE SD and 187–247°C for its PM sample. For the binary systems at the 1:1 ratio, the PM of GLI-PEG showed a small broad endothermic peak in the range of 187–234°C, while the SD sample showed three small broad endothermic peaks in 185–248°C. In the 1:3 system, there was a small endotherm within 196–213°C in PM and 182–209°C in SD, respectively. The little endothermic peaks of drug in ternary systems and binary systems at 1:1 ratio showed that drug molecules partly interacted with polymer, and amorphous form and crystalline drug co-existed in these systems.

Fourier Transform Infrared Spectroscopy for GLI and GLI-SD

The FT-IR spectrum of GLI, PEG PMs, and SDs was recorded at 40–4000 cm^{-1} as shown in Fig. 5. The characteristic absorption peaks in 3326 cm^{-1} and 3252 cm^{-1} denoted asymmetric and symmetric stretching vibrations of N–H; 1689 cm^{-1} and 1649 cm^{-1} peaks indicated asymmetric and symmetric stretching vibrations of carbonyl; and the sharp peak in 548 cm^{-1} showed the stretching vibrations of C–S bond. In addition, the asymmetric and symmetric stretching vibrations in 1341 cm^{-1} and 1163 cm^{-1} belong to S=O sulfonyl of GLI. As for the PEG polymer, there were three obvious characteristic peaks in 843 cm^{-1}, 1109 cm^{-1}, and the broad absorption peak 2885 cm^{-1}. For the curves of PMs, the vibration peaks of GLI in PMs have almost

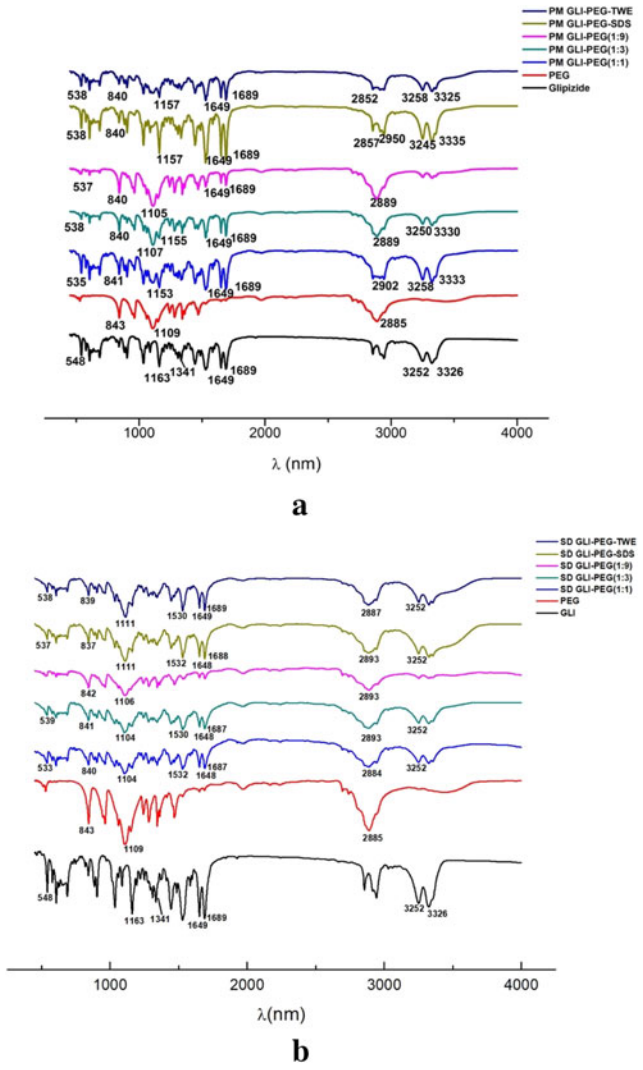

Fig. 5. IR spectrum for **a** GLI and physical mixtures; **b** GLI and solid dispersion system

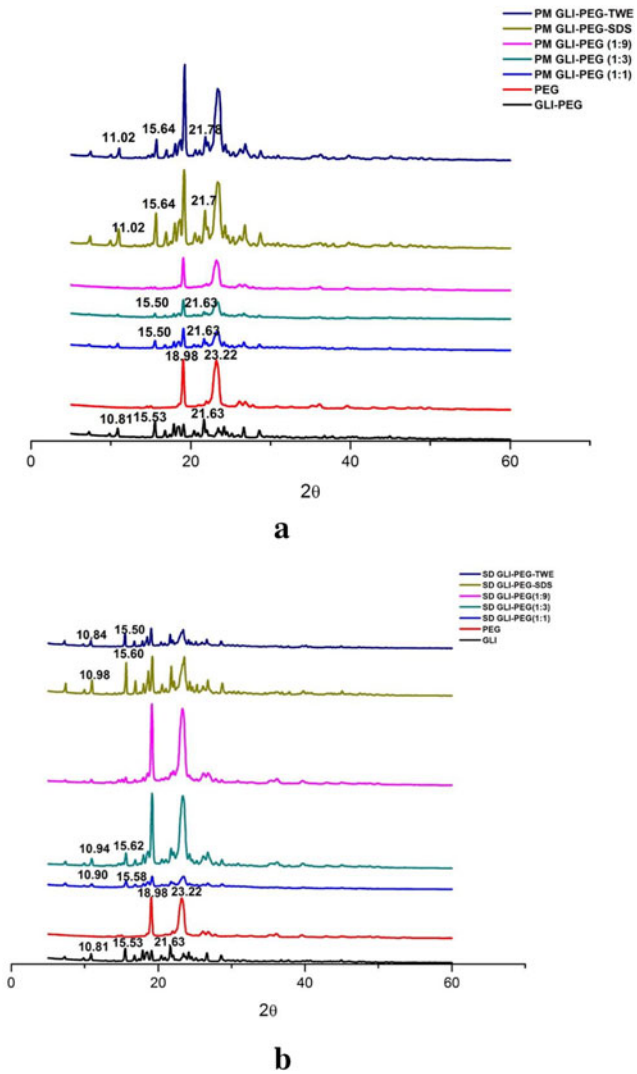

Fig. 6. XRD diagrams for **a** GLI and physical mixtures; **b** GLI and solid dispersion system

reserved, which suggested that this was simple mixture without interaction between drug molecules and polymer. There were some changes that indicated the difference between pure GLI and SD samples. The characteristic peak of sulfonyl in 1163 cm^{-1} disappeared and the intensity in 1341 cm^{-1} also decreased obviously in SD samples. On the other hand, the peak of C–S bond stretching vibration in SD showed a little bathochromic shift from 548 cm^{-1} to about 538 cm^{-1}, which indicated that the energy required for C–S vibration was less than pure drug. The absorption peaks of PEG could be observed in all SD samples but with slightly shifting and intensity decreased. The broadening, shifting, and splitting confirmed the interaction between GLI and polymer molecules.

Powder X-ray Diffraction for GLI and GLI-SD System

The XRD diagrams of pure GLI, PEG, PM, and SD samples are exhibited in Fig. 6. The crystalline feature of pure GLI was mainly characterized by diffraction peaks in the 2θ range of 7°–30°. There were obvious peaks in 10.81°, 15.53°, and 21.63°, while a small diffraction peaks occurred in 17°–20° and 23°–25°. PEG showed high intensity diffraction peaks in 19° and 23.18°. For PM sample, the diffraction peaks of pure drug and PEG could be viewed clearly except for 1:9 system. The distribution of peak intensity for each system was correlated to drug-polymer ratio. Although the characteristic peaks of GLI and PEG could also be viewed in SD samples, the intensity of GLI diffraction peaks has significantly decreased, which were also different from the PMs. Compared with pure drug, the crystalline of GLI in the ternary systems and binary system has changed partly, which indicated that drug molecules partly interacted with polymer molecules. With the polymer ratio increases, the characteristic peaks of PEG become clearer. The characteristic peaks of GLI at the 1:9 ratio cannot be found. Two possible reasons may contribute to the results: the change of drug form from crystalline to amorphous form or the increase of polymer proportion. In ternary systems, there were still very small characteristic peaks of drug crystal, which indicated that the amorphous form and crystal form co-existed in ternary systems.

Morphological Features for GLI and GLI-SDs

The SEM images of pure drug, PEG, physical mixtures, and SDs are shown in Fig. 7. Pure GLI existed as irregular-rectangle crystal form with fractured edges, while there was no regular form for PEG molecules. The crystal feature of GLI could be found in PM samples without obvious difference at each ratio. The morphology of SD samples has partly changed into amorphous form. With the percentage of PEG increased, the crystal form decreased until disappeared in 1:9 SD sample. The surface images of ternary systems exhibited some crystal form of GLI, which suggested that the solid dispersion has partly formed. SEM analysis indicated that drug molecules were homogeneously dispersed into polymer to form amorphous state in SD systems, which was the main reason for the solubilization effect of solid dispersion.

The Molecular Modeling for SD Systems

The Molecular Structure of SD Systems

The preparation process of GLI-PEG (1:1) and ternary systems were modeled by the simulated annealing method. The initial structure of GLI-PEG 1:1, GLI-PEG 1:1 + 1% SDS, and GLI-PEG 1:1 + 1% TWE is shown in Fig. 8a, b, and c, while the final structure of SD systems is exhibited in Fig. 8d, e, and f after minimization and simulated annealing process. When the drug, polymer, and surfactant molecules were conducted by Packmol program, these molecules were blended randomly with homogeneous spatial distribution. The form of initial structure was just stacked without any interaction. In the simulated annealing process, all polymers were bended and folded, while drug molecules partly inserted into polymeric coils or irregularly stick at the coil's surface.

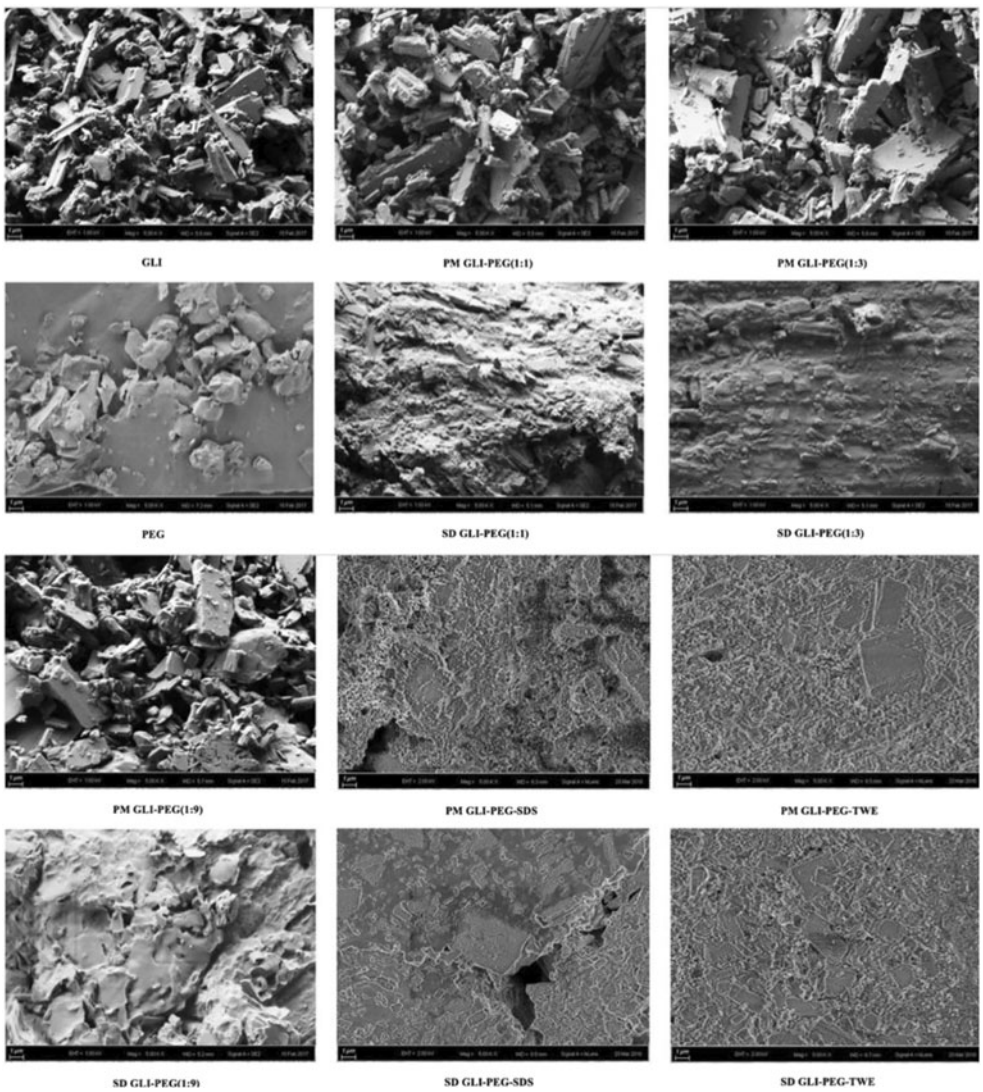

Fig. 7. Scanning electronic microscopy images of GLI, PEG, and SD systems

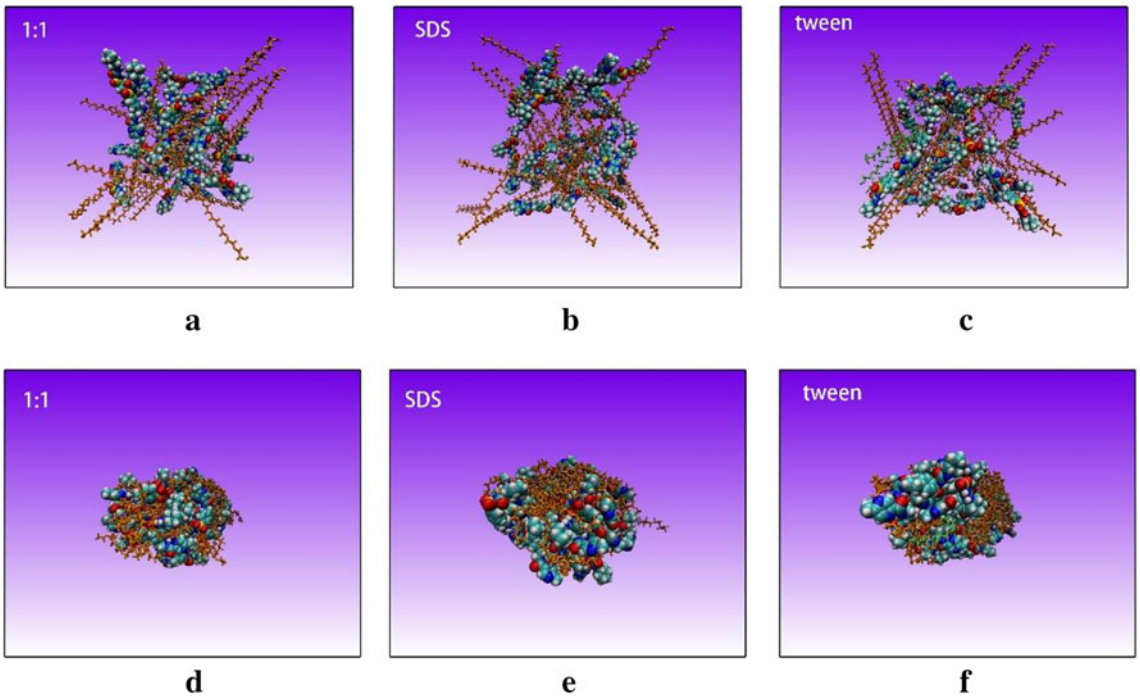

Fig. 8. The snapshots of initial structure and final structure of three SD systems

For the ternary systems, surfactant molecules were bended and wrapped with polymers as random coils, and drug molecules also dispersed in matrix. It was obvious that drug molecules could combine with polymers and surfactants with tight interaction.

The Molecular Dynamic Simulation of Dissolution Process

The systems of SD structure were immersed into dissolution medium box and conducted 300 ns MD simulation; the structures of each system at different time points were showed in Fig. 9. It provided us the dynamic dissolution process of SDs in the dissolution medium. In the first 100 ns, each system still kept the tight structure without significant change. With the simulation time increased, three systems presented different states. The 1:1 binary system always existed as twining cores, and only few polymer molecules separated from coils. In 200 ns, the twining core has divided into two parts, drug molecules also connected strongly with each other without any separation until 300 ns. For GLI-PEG-SDS ternary system, the initial structure has maintained in early 150 ns, then drug molecules started to dissociate from the whole system and release into solvent. More and more drug, polymer and surfactant molecules departed from core system, which lead to the dissolution of drug molecules. As for the GLI-PEG-TWE system, the separation of drug and polymer molecules was quickly observed in first 100 ns. The whole system was broken down and existed as friable state in 150 ns. However, the dispersed molecules re-aggregated together to form a coil again after 200 ns, then the drug molecules separated from system slowly in the later simulation process.

The final structures of these three systems after 300 ns MD simulations are shown in Fig. 10. For binary system, the spherical structure has separated into two segments, and drug molecules also bent and twined with PEG molecules in each part. There was an obvious tendency that drug and polymer molecules were separated from matrix in ternary systems, especially in SDS system. During the dissolution process of GLI-PEG-SDS system, each component dissociated from the core and then dispersed into solvent, while GLI-PEG-TWE system separated into several parts. Our modeling results were in well agreement with experimental result.

In order to describe the state during dissolution modeling, some parameters were analyzed. As Fig. 11a shows, root mean square (RMSD) of three SD systems was compared. With the time goes, three curves turned to unstable with obvious fluctuation at about 30 ns. It indicated that dissolution was the dissociation process of SDs from stable to unstable with molecular motion. In the initial stage, the RMSD of TWE ternary system was very high than the other two systems, which indicated that TWE ternary system could be dissociated rapidly with the drastic molecular motion in dissolution medium. However, there was the re-aggregation tendency for drug and polymer molecules in binary and TWE ternary system with relatively lower and stable RMSD. After 200 ns, the RMSD of GLI-PEG-SDS system was higher than that of binary system and TWE ternary system. SDS molecules prevented re-aggregation of the solute molecules. The native contact points reflected the deviation with native structure. The smaller number of native contact points indicated the dissociation process of the system. With the dissolution process proceeded, the number of native contact points of three systems were decreased until close to zero (Fig. 11b). Three curves were very close with the same tendency, indicating that the drug molecules dispersed and dissolved in medium with visible deviation from native structure. Figure 11c calculates the surface area of all solute molecules in solvent environment. The three curves maintained at the level with slight fluctuation in first 50 ns.

Fig. 9. The snapshots of SD system structures existed in the dissolution process

Then, the curve of SDS system was increased beyond another two systems, which agreed with the result of RMSD. The value of surface area showed an increase trend with fluctuation that suggested that molecules have separated from each other lead to the more surface area. These parameters also well agreed with experiments.

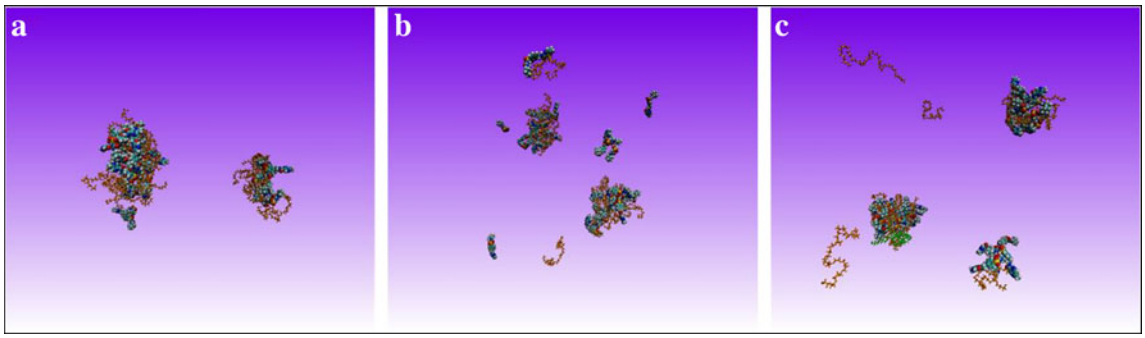

Fig. 10. The snapshots of **a** GLI-PEG 1:1, **b** GLI-PEG 1:1 + 1%SDS, **c** GLI-PEG 1:1 + 1%TWE after 300 ns MD simulation in PH7.4 phosphate buffer

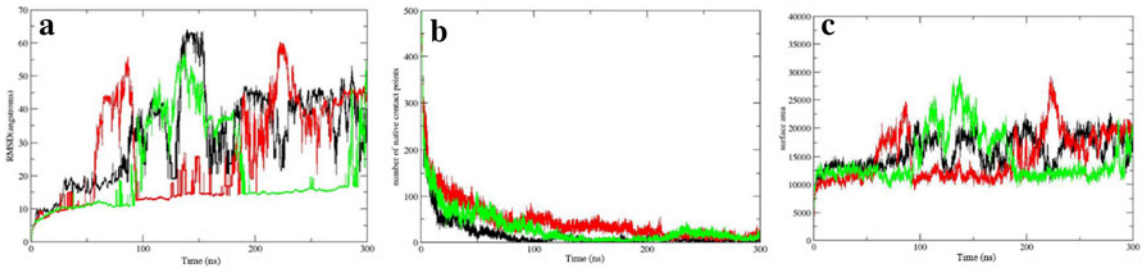

Fig. 11. Three parameters for dissolution modeling: **a** root-mean-square deviation (RMSD) curve for time; **b** the number of native contact points with time; **c** surface area ($Å^2$) of all solute molecules in the solvent fluctuated as a function of time (black is GLI-PEG system, red is GLI-PEG-SDS system, and green is GLI-PEG-TWE system)

DISCUSSION

The Tg value represents the good miscibility between drug and polymers in SD system (45). The Gordon–Taylor equation was one of the most widely used equation to calculate Tg value (46):

$$Tg = (w_1Tg_1 + kw_2Tg_2)/(w_1 + kw_2)$$

where Tg was the glass transition temperature of mixture; Tg_1 and Tg_2 were of the components; w_1 and w_2 were the mass fraction of components; K was the adjustable fitting parameter represented a semi-quantitative measure of the interaction strength between functional groups. It can be calculated as this equation:

$$K = (\rho_1 Tg_1)/(\rho_2 Tg_2)$$

where ρ_1 and ρ_2 were the densities of each component.

When the surfactants added into system, it should be considered the contribution of this third component. Compared with the G-T equation in parallel, the equation was revised as (47–49)

$$Tg = \sum_i [w_i \cdot k_i \cdot Tg_i]/\sum_i [w_i \cdot k_i]$$

In this equation, w_i was the mass fraction of each components, Tg_i was the specific Tg value, and k_i was the fitting parameter for each component that compared to the first component as standard:

$$k_i = (\rho_1 Tg_1)/(\rho_i Tg_i)$$

Table V. The comparison of experimental value and calculated value of Tg

SD system	Experimental Tg value (K)	Calculated Tg value (K)
GLI-PEG (1:1)	418.15	396.64
GLI-PEG (1:3)	411.15	364.95
GLI-PEG (1:9)	406.15	348.36
GLI-PEG-SDS (1:1:0.02)	402.15	397.49
GLI-PEG-TWE (1:1:0.02)	398.15	389.168

Note: $\rho_{GLI} = 1.29$ g/cm^3; $Tg_{GLI} = 481.15$ K; $\rho_{PEG} = 1.27$ g/cm^3; *$Tg_{PEG} = 338.15$ K; $\rho_{SDS} = 1.09$ g/cm^3; $Tg_{SDS} = 478.15$ K; $\rho_{TWE} = 1.10$ g/cm^3; $Tg_{TWE} = 148.89$ K (data were collected from PubChem website: https://pubchem.ncbi.nlm.nih.gov/)*

The values of Tg indicated the drug-polymer miscibility. A good fitness of theoretical Tg with experimental Tg indicated that the blends were miscible with weak intermolecular interaction. If theoretical Tg was larger than experimental value, there was more contribution of individual drug and/or polymer than their combination. In contrast, if theoretical value that was less than or equal to experimental value, it suggested good miscibility. In Table V, the calculated Tg value of ternary and binary SD systems was less than experimental value, which confirmed the miscibility between GLI, polymer, and surfactants at different ratios.

In our research, solid dispersions were characterized by combining experimental and molecular modeling techniques. The dissolution effect of ternary systems was better than binary system at the same ratio. Moreover, the SDS system was more efficient than TWE system. Drug molecules inserted into polymer chains or interacted at the surface, which changed the regularly arranged crystal form of GLI into amorphous form (41,42). In the dissolution process, less energy needed to dissolve drug molecules with amorphous structure. When SDs were soaked in dissolution medium, the spherical core split into severe parts, drug molecules at the surface of polymeric coils could be released into the solution.

When the surfactants added into system, dissolution behavior was better than binary system at the same ratio. Only 1% of surfactants were added, which was far away from critical micelle concentration. So the wetting effect may make a major contribution (42). Surfactants decreased the interfacial tension between solvent and SD powder. Although different surfactants have improved dissolution profiles of GLI, the anionic surfactant SDS showed better solubilization ability than non-surfactant TWE systems. During dissolution process, SDS with negative charge could well interact with solvent molecules to accelerate the disintegration of SD system. The molecular structure of nonionic surfactant TWE was relatively big with long chain, which could be twined and folded with drug and polymer molecules with strong interaction. When the TWE system was immersed into dissolution medium, more solvent could be absorbed into core and then release drug molecules because of the wetting effect. On the other hand, the strong interaction between TWE and drug or polymers made it slower dissolution than ternary system with SDS. Thus, ternary systems with surfactant were also better than binary system.

CONCLUSION

In this research, ternary solid dispersion systems with very small amount of surfactant (1%) were prepared and the dissolution mechanism was investigated at the molecular level. Ternary SD showed significant better dissolution ability than binary system at the same polymer ratio, even 1% surfactants leading to the significant solubilization effect. Combined experimental and molecular modeling techniques were the novel strategy to solve the issues of solid dispersions. The integrated experimental and molecular modeling methodology is able to greatly benefit for the formulation development in the future.

FUNDING INFORMATION

Current research is financially supported by the University of Macau Research Grant (MYRG2016-00040-ICMS-QRCM) and the 2017 Sub-project 6 of National Major Scientific and Technological Special Project for “Significant New Drugs Development” of the Ministry of Science and Technology of China (2017ZX09101001006). Molecular modeling was performed in part at the High-Performance Computing Cluster (HPCC) which is supported by Information and Communication Technology Office (ICTO) of the University of Macau.

REFERENCES

1. Kawabata Y, Wada K, Nakatani M, Yamada S, Onoue S. Formulation design for poorly water-soluble drugs based on biopharmaceutics classification system: basic approaches and practical applications. Int J Pharm. 2011;420(1):1–10.
2. Renuka, Singh SK, Gulati M, Narang R. Stable amorphous binary systems of glipizide and atorvastatin powders with enhanced dissolution profiles: formulation and characterization. Pharm Dev Technol. 2017;22(1):13–25.
3. Löbenberg R, Amidon GL. Modern bioavailability, bioequivalence and biopharmaceutics classification system. New scientific approaches to international regulatory standards. Eur J Pharm Biopharm. 2000;50(1):3–12.
4. Food, Administration D. Guidance for industry: waiver of in vivo bioavailability and bioequivalence studies for immediate-release solid oral dosage forms based on a biopharmaceutics classification system. Food and Drug Administration, Rockville, MD. 2000.
5. Sun DD, Lee PI. Evolution of supersaturation of amorphous pharmaceuticals: the effect of rate of supersaturation generation. Mol Pharm. 2013;10(11):4330–46.
6. Verma S, Rudraraju VS. Wetting kinetics: an alternative approach towards understanding the enhanced dissolution rate for amorphous solid dispersion of a poorly soluble drug. AAPS PharmSciTech. 2015;16(5):1079–90.
7. Huang Y, Dai W-G. Fundamental aspects of solid dispersion technology for poorly soluble drugs. Acta Pharm Sin B. 2014;4(1):18–25.
8. Pouton CW. Formulation of poorly water-soluble drugs for oral administration: physicochemical and physiological issues and the lipid formulation classification system. Eur J Pharm Sci. 2006;29(3):278–87.
9. Baghel S, Cathcart H, O’Reilly NJ. Investigation into the solid-state properties and dissolution profile of spray-dried ternary amorphous solid dispersions: a rational step toward the design and development of a multicomponent amorphous system. Mol Pharm. 2018;15:3796–812.
10. Park J-B, Park C, Piao ZZ, Amin HH, Meghani NM, Tran PH, et al. pH-independent controlled release tablets containing nanonizing valsartan solid dispersions for less variable bioavailability in humans. J Drug Deliv Sci Tec. 2018;46:365–77.
11. Orlandi S, Priotti J, Diogo HP, Leonardi D, Salomon CJ, Nunes TG. Structural elucidation of Poloxamer 237 and Poloxamer 237/Praziquantel solid dispersions: impact of poly (Vinylpyrrolidone) over drug recrystallization and dissolution. AAPS PharmSciTech. 2018;19(3):1274–86.
12. Lehmkemper K, Kyerematen SO, Degenhardt M, Sadowski G. Influence of low-molecular-weight excipients on the phase behavior of pvpva64 amorphous solid dispersions. Pharm Res. 2018;35(1):25.
13. Alhayali A, Tavellin S, Velaga S. Dissolution and precipitation behavior of ternary solid dispersions of ezetimibe in biorelevant media. Drug Dev Ind Pharm. 2017;43(1):79–88.

14. Deshpande TM, Shi H, Pietryka J, Hoag SW, Medek A. Investigation of polymer/surfactant interactions and their impact on Itraconazole solubility and precipitation kinetics for developing spray-dried amorphous solid dispersions. Mol Pharm. 2018;15(3):962–74.
15. Li M, Ioannidis N, Gogos C, Bilgili E. A comparative assessment of nanocomposites vs. amorphous solid dispersions prepared via nanoextrusion for drug dissolution enhancement. Eur J Pharm Biopharm. 2017;119:68–80.
16. Segale L, Giovannelli L, Mannina P, Pattarino F. Formulation and characterization study of itraconazole-loaded microparticles. Pharm Dev Technol. 2015;20(2):153–8.
17. Pongpeerapat A, Itoh K, Tozuka Y, Moribe K, Oguchi T, Yamamoto K. Formation and stability of drug nanoparticles obtained from drug/PVP/SDS ternary ground mixture. J Drug Deliv Sci Tec. 2004;14(6):441–7.
18. Rao JV, Pore YV, Shinde VR. Development and characterization of ternary solid dispersion systems of olmesartan medoxomil. Lat Am J Pharm 2011;30.
19. El Maghraby GM, Alomrani AH. Effect of binary and ternary solid dispersions on the in vitro dissolution and in situ rabbit intestinal absorption of gliclazide. Pak J Pharm Sci. 2011;24(4):459–68.
20. Zaki RM, Ali AA, El Menshawi SF, Bary AA. Effect of binary and ternary solid dispersions prepared by fusion method on the dissolution of poorly water soluble diacerein. Int J Drug Deliv. 2013;5(1):99–109.
21. Wang H, Xu HX, Zhang N, Hu LD, editors. Enhancement of Dissolution Rate of Daidzein in Ternary Solid Dispersions. Adv Mater Res; 2012: Trans Tech Publ.
22. Kadir MF, Sayeed MSB, Khan RI, Shams T, Islam MS. Study of binary and ternary solid dispersion of ibuprofen for the enhancement of oral bioavailability. JAPS. 2011;1(9):13.
23. Kadir MF, Alam MR, Rahman AB, Jhanker YM, Shams T, Khan RI. Study of binary and ternary solid dispersion of spironolactone prepared by co-precipitation method for the enhancement of Oral bioavailability. JAPS. 2012;2(10):117.
24. Li J, Liu P, Liu J-P, Zhang W-L, Yang J-K, Fan Y-Q. Novel Tanshinone II a ternary solid dispersion pellets prepared by a single-step technique: in vitro and in vivo evaluation. Eur J Pharm Biopharm. 2012;80(2):426–32.
25. Jung HJ, Ahn HI, Park JY, Ho MJ, Lee DR, Cho HR, et al. Improved oral absorption of tacrolimus by a solid dispersion with hypromellose and sodium lauryl sulfate. Int J Biol Macromol. 2016;83:282–7.
26. Mura P, Moyano J, González-Rodríguez M, Rabasco-Alvarez A, Cirri M, Maestrelli F. Characterization and dissolution properties of ketoprofen in binary and ternary solid dispersions with polyethylene glycol and surfactants. Drug Dev Ind Pharm. 2005;31(4–5):425–34.
27. Goddeeris C, Willems T, Houthoofd K, Martens J, Van den Mooter G. Dissolution enhancement of the anti-HIV drug UC 781 by formulation in a ternary solid dispersion with TPGS 1000 and Eudragit E100. Eur J Pharm Biopharm. 2008;70(3):861–8.
28. Cirri M, Maestrelli F, Corti G, Mura P, Valleri M. Fast-dissolving tablets of glyburide based on ternary solid dispersions with PEG 6000 and surfactants. Drug Deliv. 2007;14(4):247–55.
29. Janssens S, Nagels S, De Armas HN, D'autry W, Van Schepdael A, Van den Mooter G. Formulation and characterization of ternary solid dispersions made up of Itraconazole and two excipients, TPGS 1000 and PVPVA 64, that were selected based on a supersaturation screening study. Eur J Pharm Biopharm. 2008;69(1):158–66.
30. Goddeeris C, Willems T, Van den Mooter G. Formulation of fast disintegrating tablets of ternary solid dispersions consisting of TPGS 1000 and HPMC 2910 or PVPVA 64 to improve the dissolution of the anti-HIV drug UC 781. Eur J Pharm Sci. 2008;34(4–5):293–302.
31. Wang X, Michoel A, Van den Mooter G. Solid state characteristics of ternary solid dispersions composed of PVP VA64, Myrj 52 and itraconazole. Int J Pharm. 2005;303(1–2):54–61.
32. Mura P, Faucci M, Manderioli A, Bramanti G, Parrini P. Thermal behavior and dissolution properties of naproxen from binary and ternary solid dispersions. Drug Dev Ind Pharm. 1999;25(3):257–64.
33. Riekes MK, Engelen A, Appeltans B, Rombaut P, Stulzer HK, Van den Mooter G. New perspectives for fixed dose combinations of poorly water-soluble compounds: a case study with ezetimibe and lovastatin. Pharm Res. 2016;33(5):1259–75.
34. Bhise SD. Ternary solid dispersions of fenofibrate with poloxamer 188 and TPGS for enhancement of solubility and bioavailability. Int J Res Pharmaceut Biomed Sci. 2011;2(2):583–95.
35. Dave RH, Patel HH, Donahue E, Patel AD. To evaluate the change in release from solid dispersion using sodium lauryl sulfate and model drug sulfathiazole. Drug Dev Ind Pharm. 2013;39(10):1562–72.
36. Khaleel NY, Abdulrasool AA, Ghareeb MM, Hussain SA. Solubility and dissolution improvement of ketoprofen by solid dispersion in polymer and surfactant using solvent evaporation method. Acad Sci IJPPS. 2011;3:431–5.
37. Schlick T. Molecular modeling and simulation: an interdisciplinary guide: an interdisciplinary guide: Springer Science & Business Media; 2010.
38. De Vivo M, Masetti M, Bottegoni G, Cavalli A. Role of molecular dynamics and related methods in drug discovery. J Med Chem. 2016;59(9):4035–61.
39. Ouyang D, (Eds.) SCS. Computational Pharmaceutics: Application of Molecular Modeling in Drug Delivery: John Wiley & Sons Ltd., Chichester, West Sussex, United Kingdom, Hoboken(Book); 2015.
40. Ouyang D. Investigating the molecular structures of solid dispersions by the simulated annealing method. Chem Phys Lett. 2012;554:177–84.
41. Chan T, Ouyang D. Investigating the molecular dissolution process of binary solid dispersions by molecular dynamics simulations. AJPS. 2018;13(3):248–54.
42. Chen W, Ouyang D. Investigation of molecular dissolution mechanism of ketoprofen binary and ternary solid dispersions by molecular dynamics simulations. Mol Simul. 2017;43(13–16):1074–80.
43. Yale J-F. Oral antihyperglycemic agents and renal disease: new agents, new concepts. J Am Soc Nephrol. 2005;16(3 suppl 1):S7–S10.
44. Kirkpatrick S, Gelatt CD, Vecchi MP. Optimization by simulated annealing. Science. 1983;220(4598):671–80.
45. Kennedy M, Hu J, Gao P, Li L, Ali-Reynolds A, Chal B, et al. Enhanced bioavailability of a poorly soluble VR1 antagonist using an amorphous solid dispersion approach: a case study. Mol Pharm. 2008;5(6):981–93.
46. Gordon M, Taylor JS. Ideal copolymers and the second-order transitions of synthetic rubbers. I. Non-crystalline copolymers. J Appl Chem. 1952;2(9):493–500.
47. Bliznyuk V, Assender H, Briggs G. Surface glass transition temperature of amorphous polymers. A new insight with SFM. Macromolecules. 2002;35(17):6613–22.
48. Boller A, Schick C, Wunderlich B. Modulated differential scanning calorimetry in the glass transition region. Thermochim Acta. 1995;266:97–111.
49. Abiad M, Carvajal M, Campanella O. A review on methods and theories to describe the glass transition phenomenon: applications in food and pharmaceutical products. Food Eng Rev. 2009;1(2):105–32.